Journal of Vertebrate Paleontology 28(3):826–840, September 2008


ARTICLE

# A NEW CLADE OF OMOMYID PRIMATES FROM THE EUROPEAN PALEOGENE

J. J. HOOKER,[*,1] and D. L. HARRISON[2]
[1]Department of Palaeontology, Natural History Museum, Cromwell Road, London, SW7 5BD, United Kingdom, j.hooker@nhm.ac.uk;
[2]Harrison Institute, Centre for Systematics and Biodiversity Research, Bowerwood House, St Botolph's Road, Sevenoaks, Kent, TN13 3AQ, United Kingdom, harrisoninstitute@btopenworld.com

ABSTRACT—A new genus, *Vectipithex*, is erected in the subfamily Microchoerinae, family Omomyidae, for four species, of which one, the type species is new: *V. smithorum* sp. nov. '*Protoadapis*' *ulmensis* is referred to *Vectipithex* and transferred from the family Adapidae. Two species of *Nannopithex*, '*N.*' *quaylei* and '*N.*' *raabi* are also referred to the new genus. *Vectipithex* has a geographic distribution in north and west Europe and a stratigraphic distribution from the early Middle Eocene (Lutetian) to latest Eocene (late Priabonian). Cladistic analysis shows that *Vectipithex* is sister group to a clade composed of *Microchoerus*, *Necrolemur*, *Nannopithex filholi*, and '*N.*' *zuccolae* and that poorly known '*N.*' *humilidens* is sister group to those two. The Microchoerinae are shown to have undergone a phase of rapid diversification in the first few million years of the Eocene.

## INTRODUCTION

The species *Adapis ulmensis* Schmidt-Kittler, 1971 was named for a well preserved m1 (holotype) and two fragmentary and rolled lower cheek teeth identified as p4 and p3 (paratypes), from the fissure filling of Ehrenstein 1, Bavaria, southern Germany. Ehrenstein 1 has mixed faunas of two ages (Schmidt 1969), one dated as Late Eocene (Mammalian Paleogene reference level MP18), the other as Early Oligocene (MP21) (Brunet et al. 1987). The earlier fauna has been referred to as Ehrenstein 1(A), the later one as Ehrenstein 1(B). In 1971, because there was no consensus on the position of the Eocene-Oligocene boundary, the Ehrenstein 1(A) fauna was dated as Early Oligocene. Schmidt-Kittler (1977) described more cheek teeth belonging to *A. ulmensis* from Ehrenstein 1 and contemporaneous Ehrenstein 3 and Herrlingen 3 in the same area. These teeth consisted of P3, M1, incomplete M3, and m3. These new specimens showed that the species differed significantly from other species of *Adapis* and Schmidt-Kittler (1977) referred *A. ulmensis* to the genus *Protoadapis* Lemoine, 1878. Two teeth from the contemporaneous Ehrenstein 2 fissure filling were identified as m1 and M3 of 'Adapidae sp.' (Schmidt-Kittler 1977, figs. 6, 7). The m1 is re-identified here as dp4 and both teeth are attributed also to *P. ulmensis*.

Well preserved upper and lower cheek teeth collected by comprehensive screenwashing to 0.5 mm from several levels in the Late Eocene Headon Hill and Bembridge Limestone Formations of the Hampshire Basin, southern England bear a striking resemblance to those of *P. ulmensis*. These have been referred to this species in faunal lists, sometimes with some qualification as to both genus and species (Hooker 1989, 1992, Hooker et al. 1995, 2004, 2005). They are here named as a new species. Additionally, tooth loci of this new species include ones not recognised in the Bavarian sites. These comprise enlarged upper and lower first incisors, greatly reduced i2, and simplified and procumbent I2, upper and lower canines, p3 and p4. Their morphology indicates referral of '*P.*' *ulmensis* and the new species to the subfamily Microchoerinae, family Omomyidae (see e.g. Thalmann 1994) rather than to the family Adapidae.

*Nannopithex quaylei* Hooker, 1986 was named for an M2 (holotype) and several other isolated teeth (paratypes), identified as I1, P4, M3, i1, p3, m1/2, and m3, from the late Middle Eocene (Bartonian) Creechbarrow Limestone Formation of Creechbarrow, Dorset, Hampshire Basin. The p3 of *N. quaylei* is here reidentified as the lower canine. According to a 'manual' cladistic analysis of the Microchoerinae (Hooker 1986: 263–269), *Nannopithex* Stehlin, 1916 was seen to be paraphyletic, some species being related to *Pseudoloris* Stehlin, 1916, one to be stem member of the whole subfamily, and the type species to be stem member of a clade consisting of *Necrolemur* Filhol, 1873 and *Microchoerus* Wood, 1844. Thalmann (1994) reanalysed the Microchoerinae cladistically using PAUP 3.0 and concluded that *N. quaylei* was sister taxon to *N. abderhaldeni* (Weigelt, 1933) from Geiseltal. *N. abderhaldeni* has rather consistently been synonymised with *N. raabi* (Heller, 1930) (Simons 1961, Szalay and Delson 1979, Hooker 1986), while Gunnell and Rose (2002) recognised only *N. raabi* and *N. humilidens* Thalmann, 1994 as valid species from Geiseltal, by implication synonymising both *N. abderhaldeni* and *N. barnesi* Thalmann, 1994 with *N. raabi*. Another species of *Nannopithex*, *N. zuccolae* Godinot, Russell and Louis, 1992 from the late Early Eocene (late Ypresian) of the Paris Basin, has been placed close to *N. filholi* (Chantre and Gaillard, 1897) and the *Necrolemur—Microchoerus* clade (see Thalmann 1994).

An important difference between *N. raabi* on the one hand and *N. filholi* and *N. zuccolae* on the other is the absence of P2 in the former (Thalmann 1994). Moreover, no P2 has been recovered for the new species, despite the finding of all the other tooth loci that are present in *N. raabi*. New finds of *N. quaylei* at Creechbarrow have likewise yielded all the tooth loci present in *N. raabi* except p3, but again no P2. Reconstruction of the upper and lower dentitions of *N. quaylei* and the new species according to their occlusal relationships (see below) shows rather elongate

[*]Corresponding author.

upper canine and I2, leaving no room for P2, and showing an occlusal pattern very similar to that of *N. raabi* (see Thalmann 1994, fig.3.10a). The close relationship of *N. raabi*, *N. quaylei*, '*Protoadapis*' *ulmensis*, and the new species is indicative of a distinct clade within the Microchoerinae, which warrants a new generic name.

**Institutional Abbreviations**—**BMNH**, Natural History Museum, London, UK; **BSPG**, Bayerische Staatssammlung für Paläontologie und historisches Geologie, Munich, Germany; **BU**, Bristol University, UK; **GMH**, Geiseltal Museum, Halle, Germany; **HZM**, Harrison Institute, Sevenoaks, UK; **SMNS**, Staatliches Museum für Naturkunde, Stuttgart, Germany.

**Synonymy Notation**—This follows Matthews (1973), such that: '*' = valid type citation; '.' = the reference pertains to the species under discussion; '?' = there is doubt whether the reference pertains to the species under discussion; 'non' = the reference does not pertain to the species under discussion; 'p' = the reference pertains only in part to the species under discussion; 'v' = we have seen the specimens involved.

## SYSTEMATIC PALEONTOLOGY

Order PRIMATES Linnaeus, 1758
Infraorder TARSIIFORMES? Gregory, 1915
Family OMOMYIDAE Trouessart, 1879
Subfamily MICROCHOERINAE Lydekker, 1887
Genus *VECTIPITHEX* nov.

**Type Species**—*Vectipithex smithorum* sp. nov., from the Headon Hill and Bembridge Limestone Formations, Priabonian, Eocene, Headon Hill, Isle of Wight, England.

**Included Species**—*V. ulmensis* (Schmidt-Kittler, 1971) comb. nov., *V. quaylei* (Hooker, 1986) comb. nov., *V. raabi* (Heller, 1930) comb. nov.

**Etymology**—From *Vectis*, the Roman name for the Isle of Wight, and the Greek *pithex*, monkey, a suffix used elsewhere for a microchoerine genus.

**Occurrence**—Lutetian (Mammalian Paleogene reference level MP13, Geiseltalian European Land Mammal Age) to late Priabonian (MP19, Headonian ELMA), Eocene, of Germany and England.

**Diagnosis**—Microchoerines with dental formula: 2123/2123, thus lacking P2. Presence of M1–2 lingual cingulum, which may be interrupted at the protocone (paralleled in the interrupted state only by *Nannopithex filholi*). Lower m3 talonid basal plane angled up with respect to that of the trigonid (paralleled by *Melaneremia* Hooker, 2007 and *Pseudoloris*). Lacks the derived characters of mesiolingual crest on paracone of upper cheek teeth and on main cusp of upper incisors and canine, consistent strong enamel wrinkling, unwaisted P3 protocone lobe, paracone-protocone crest on P3–4, broken upper molar postprotocrista, large M1–2 hypocone, closed m1 trigonid, mesial m1 metaconid crest, and wide m3 hypoconulid lobe present in *Necrolemur*, *Microchoerus*, and to a greater or lesser extent in *Nannopithex filholi* and '*N.*' *zuccolae*. Lacks the derived high m1–2 entoconid of *Pseudoloris* and '*N*'. *humilidens* and the long M1–2 postmetacrista of *Pseudoloris*. *Melaneremia* differs in lacking enamel wrinkling and in having M1/2 with distinct postcingulum and metacingulum and without lingual cingulum, symmetrical p4 with long talonid and lower paraconid and relatively narrow third molars with lingually non-salient m3 entoconid. In addition to these differences, *Paraloris* Fahlbusch, 1995 has the p4 distal wall sloping occusodistally.

**Remarks**—Although *V. ulmensis* is represented by relatively few tooth loci, their similarity to those of *V. smithorum* imply the absence of P2 in this species too. *V. raabi* is the least derived species of the genus, the most distinctive characters of elongate and procumbent anterior teeth, and the adapid-like lack of a *Nannopithex* fold, complete postprotocrista, and complete lingual cingulum on M1–2 being evolved in the more derived species.

### *VECTIPITHEX SMITHORUM* sp. nov.
(Figs. 1E–I, T, Z–AA, 2H–O, 3H–N, P)

v. 1987 *Protoadapis* cf. *ulmensis* (Schmidt-Kittler): Hooker:113.
v. 1989 *Protoadapis ?ulmensis* (Schmidt-Kittler): Hooker:17.
v. 1992 *Protoadapis ulmensis* (Schmidt-Kittler): Hooker:513.
v. 1995 '*Protoadapis*' *ulmensis* (Schmidt-Kittler): Hooker et al.: 454.
v. 2004 '*Protoadapis*' *ulmensis* (Schmidt-Kittler): Hooker et al.: 163.
v. 2005 *Protoadapis ulmensis* (Schmidt-Kittler): Hooker et al.: 108.

**Holotype**—Associated left i1, p4, m2, m3, right i1, i2 (BMNH.M45654) from clay in How Ledge Limestone, Totland Bay Member, Headon Hill Formation (= Bosma's 1974 sampling point HH2), early Priabonian, Eocene, Headon Hill, Isle of Wight, UK. (See Daley 1999 for Headon Hill Formation stratigraphy).

**Paratypes**—Associated right I1, C, M1, M3 (fragment) (SMNS.42461); possibly associated left P3 and buccal half of P4 (SMNS.42450); associated right p4 (HZM.7.21894), m1 (HZM.8.21895), m2 (HZM.9.21896), m3 (HZM.10.21897); right M3 (HZM.25.29435); unworn left M1 (HZM.4.19545); unworn right m3 (HZM.1.18951); all from the same horizon and locality as the holotype. Associated right I2, upper canine, M2 (fragment), i1, c (fragment), p3, m1, m2 trigonid (BMNH.M45657) from the top of the Hatherwood Limestone Member, Headon Hill Formation, middle Priabonian, Headon Hill. Associated left and right I1s, upper canine, P3 (fragment), P4 (fragments), M1 (fragment), M2, c, m1, m3 (BMNH.M52036, M52465) from beds 15/18, Bembridge Limestone Formation, late Priabonian, Headon Hill (bed numbers from Hooker et al. 1995).

**Referred Specimens**—Right I2 (BMNH.M45655), right C (BMNH.M62125), right P4 buccal half (HZM.29.29670), left M1 (HZM.28.29669), right M1 (HZM.24.29434), left M3 (HZM.26.29450), right p3 (BMNH.M61303), left m1 trigonid (HZM.31.29784), right m1 trigonid (HZM.12.22579), enamelless right m2 (BMNH.M62126); from the same horizon and locality as the holotype. Right M1 (BU.23337), right M2 and left M3 (BU.23275), from clay in How Ledge Limestone, Totland Bay Member, Headon Hill Formation (= Bosma's 1974 sampling point TB), Totland Bay, Isle of Wight. Fragmentary left M1 (HZM.23.29269) from the rodent bed, Totland Bay Member, Hordle Cliff, Hampshire (see Edwards and Daley 1997, for stratigraphy). Left M2 (HZM.13.26162), left m3 (HZM.11.22556); from shell bed at base of lignite bed, Hatherwood Limestone Member, Headon Hill Formation (= Bosma's 1974 sampling point HH3), Headon Hill. Left upper canine (BMNH.M53210), left M3 (BMNH.M53211), from bed 5; right i1 (HZM.15.27072), from bed 10; left c (BMNH.M52034), from bed 18; right M1 (HZM.5.19672); all Bembridge Limestone Formation, Headon Hill.

**Etymology**—After John and Marion Smith, who provided friendly access to their cliffs below Headon Hall, where some of the specimens described here were found, and were helpful in many other ways.

**Diagnosis**—Large species of *Vectipithex*, mean M1 length: 3.64 mm; mean m1 length: 4.00 mm. Mean length of M1 is 77.5 percent of width (range 74–79 percent); mean length of m1 is 136.5 percent of width (range 131–141 percent) (Table 1). I1 crown base obliquely oriented with respect to root. i1 long axis oriented at c. 30 degrees to cheek tooth row. p4 without lingually salient paraconid and with basal crown margin angled up mesial of the metacone. *Vectipithex ulmensis* is slightly larger with first

TABLE 1. Measurements in millimeters of measurable teeth of *Vectipithex smithorum*, *V. ulmensis*, and *V. quaylei*.

| | | Length | | | Width | | L/W | |
|---|---|---|---|---|---|---|---|---|
| Tooth | N | OR | Mean | N | OR | Mean | OR | Mean |
| *V. smithorum* | | | | | | | | |
| I1 | 2 | 2.89–3.09 | 2.99 | 1 | 2.23 | | 1.31 | |
| I2 | 2 | 2.44–2.57 | 2.51 | 2 | 1.55–1.77 | 1.66 | 1.45–1.57 | 1.51 |
| C | 4 | 3.57–4.03 | 3.77 | 4 | 1.63–1.89 | 1.78 | 1.92–2.24 | 2.12 |
| P3 | 1 | 3.15 | | 1 | 2.94 | | 1.07 | |
| P4 | 2 | 3.14–3.21 | 3.18 | | | | | |
| M1 | 4 | 3.54–3.91 | 3.74 | 6 | 4.46–5.00 | 4.70 | 0.78–0.79 | 0.79 |
| M2 | 3 | 3.43–3.58 | 3.52 | 3 | 4.74–5.08 | 4.87 | 0.71–0.74 | 0.72 |
| M3 | 4 | 2.46–3.14 | 2.94 | 2 | 4.08–4.31 | 4.20 | 0.71–0.76 | 0.74 |
| i1 | 2 | 2.97–3.20 | 3.09 | 2 | 2.17–2.29 | 2.23 | 1.37–1.40 | 1.39 |
| i2 | 2 | 1.34–1.51 | 1.43 | 2 | 1.40–1.49 | 1.45 | 0.96–1.01 | 0.99 |
| c | 2 | 2.77–2.80 | 2.79 | 2 | 1.69–1.83 | 1.76 | 1.51–1.66 | 1.59 |
| p3 | 2 | 2.03–2.56 | 2.30 | 2 | 1.43–1.72 | 1.58 | 1.42–1.49 | 1.46 |
| p4 | 2 | 3.12–3.17 | 3.15 | 2 | 2.46–2.60 | 2.53 | 1.20–1.29 | 1.25 |
| m1 | 4 | 3.54–4.29 | 4.00 | 4 | 2.51–3.14 | 2.94 | 1.31–1.41 | 1.37 |
| m2 | 2 | 3.83–3.90 | 3.87 | 2 | 3.11–3.24 | 3.18 | 1.20–1.23 | 1.22 |
| m3 | 5 | 3.63–4.39 | 4.02 | 5 | 2.40–2.76 | 2.56 | 1.51–1.65 | 1.57 |
| dp4 | 1 | 3.31 | | 1 | 2.20+ | | | |
| *V. ulmensis* | | | | | | | | |
| P3 | 1 | 3.97 | | 1 | 3.69 | | 1.08 | |
| M1 | 1 | 4.11 | | 1 | 4.97 | | 0.83 | |
| M2 | | | | 2 | 5.14–5.43 | 5.29 | | |
| M3 | 1 | 3.03 | | 1 | 3.89 | | 0.78 | |
| m1 | 1 | 4.63 | | 1 | 3.09 | | 1.50 | |
| m2 | 1 | 4.06+ | | 1 | 3.14 | | 1.29+ | |
| dp4 | 1 | 3.66 | | 1 | 2.46 | | 1.49 | |
| *V. quaylei* | | | | | | | | |
| I1 | 5 | 1.78–2.34 | 2.07 | 5 | 1.18–1.80 | 1.44 | 1.30–1.51 | 1.44 |
| I2 | 3 | 2.00–2.26 | 2.11 | 2 | 1.20–1.40 | 1.30 | 1.47–1.67 | 1.57 |
| C | 1 | 2.90 | | 1 | 1.44 | | 2.01 | |
| P3 | 2 | 2.60–(2.74) | (2.67) | 2 | 2.57–2.91 | 2.74 | (0.94)–1.01 | (0.98) |
| P4 | 3 | 2.34–2.69 | 2.55 | 1 | 3.60 | | 0.73 | |
| M1 | 1 | 2.70 | | | | | | |
| M2 | 1 | 2.71 | | 1 | 3.86+ | | <0.70 | |
| i1 | 1 | 2.63 | | 1 | 1.72 | | 1.53 | |
| i2 | 1 | 1.20 | | 1 | 1.06 | | 1.13 | |
| c | 1 | 2.26 | | 1 | 1.40 | | 1.61 | |
| p4 | 1 | 2.60 | | | | | | |
| m2 | 1 | 3.06 | | 2 | 2.40–2.41 | 2.41 | 1.28 | |
| m3 | 3 | 3.03–3.43 | 3.26 | 4 | 1.43–2.06 | 1.79 | 1.61–1.87 | 1.71 |
| dp4 | | | | 1 | 1.56 | | | |

For first incisors, length is anteroposterior, width is mediolateral; for all other teeth, length is mesiodistal, width is buccolingual (see text).
**Abbreviations**: **N**, number; **OR**, observed range.

molars having greater length-width proportions. *V. quaylei* and *V. raabi* are smaller with lesser length-width proportions of upper molars, I1 with more symmetrical crown. *V. quaylei* and *V. raabi* have M2 with *Nannopithex* fold, and p4 with basal crown margin straight on the lingual side, and paraconid salient lingually. *V. raabi* has M1 with *Nannopithex* fold and i1 long axis at c. 40 degrees to cheek tooth row.

## Description

**I1**—Anterior and posterior are used specifically here because, whereas the posterior direction equates with distal, anterior does not equate with mesial. By analogy with *Microchoerus erinaceus* Wood, 1844, the buccal surface bends nearly at right angles within I1 (Fig. 1E1). In lateral view this tooth is only slightly taller (base to apex) than long (anteroposterior) (Fig. 2H1). The enamel edge of the crown base is slightly oblique to the crown long axis and the anterior crown margin subtends an acute angle to the root long axis, bending more substantially as it nears the main cusp tip. Posteriorly, there is a basal crown swelling forming a blunt heel. A faint interstitial facet for I2 marks the posterior side of the heel, but there is no visible mesial interstitial facet. This implies that like *Microchoerus* (Wood 1846, pl. 2, figs. 1, 1b), there is a gap between the I1s. Medially, the main cusp forms a blunt rib (Fig. 3I4), but without forming the crest that occurs in *Necrolemur* and *Microchoerus* (e.g. Hooker 1986). The medial surface is very slightly concave in occlusal view (Fig. 1-E1). An anteromedial crest leads from the tip of the main cusp to the mesial edge, where it recurves to form an initially high cingulum, which steps basally about a third of the distance from the anterior margin.

**I2**—The crown is much longer than wide, thus longer than in *V. raabi* and other microchoerine genera. The outline in occlusal view shows a broadly convex buccal margin and a straighter lingual margin, which bends buccally near the distal margin, forming an angled distolingual bulge (Fig. 1F1). There is a single, distally originating root (Fig. 2I1), whose cross section is transversely elongate. The crown is procumbent with a low main cusp that has concave sides flaring buccally and lingually to a broad basal region. The main cusp is slightly mesial of the midline and the occlusal edge in buccal or lingual profile shows an obtuse angle with a distinctly protruding mesial lobe. The main cusp shows a faint, vertically oriented rib on the lingual face. The distal crest is slightly concave. There is a strong lingual cingulum (Fig. 3L2), but no buccal cingulum. A tiny patch of abrasion mesiobasally appears to be the mesial interstitial facet. The distal interstitial facet for contact with the upper canine slopes at a lesser angle than the mesial one, parallel with the distal face of


FIGURE 1. Scanning electron micrographs of gold palladium-coated epoxy casts of teeth of *Vectipithex* and Adapinae? indet. in occlusal view, shown as from left side. **A**–**D**, **U**, **W**–**Y**, *V. ulmensis*. **E**–**I**, **T**, **Z**, **AA**, *V. smithorum*. **J**–**S**, **AB**–**AH**, *V. quaylei*. **V**, Adapinae? indet., p4?, paratype of '*Adapis*' *ulmensis*. Teeth are: I1 (**E1**, **J**), I2 (**F1**, **K**), C (**F2**, **L**), P3 (**A**, **G1**, **M**), P4 (**E2**, **G2**, **N**), M1 (**B**, **H**, **O**-**P**), M2 (**C**, **E3**, **Q**), M3 (**D**, **I**, **R**), i1 (**Z1**, **AB**), i2 (**Z2**, **AC**), c (**E4**, **AD**), p3 (**F3**), p4 (**Z3**, **AE**), m1 (**W**, **AA**, **AF**), m2 (**X**, **Z4**, **AG**), m3 (**Y**, **Z5**, **AH**), dp4 (**S**–**U**). **A**, BSPG.1971 XXIV-4. **B**, BSPG.1971 XXIV-1. **C**, BSPG.1968 VII-1019. **D**, BSPG.1971 XXVI-1. **E**, BMNH.M52036. **F**, BMNH.M45657. **G**, SMNS.42450. **H**, HZM.4.19545. **I**, HZM.25.29435. **J**, HZM.4.31107. **K**, HZM.13.36684. **L**, BMNH.M36216. **M**, HZM.21.37620. **N**, BMNH.M35760. **O**, HZM.17.36927. **P**, BMNH.M37692. **Q**, BMNH.M37145, holotype of *V. quaylei*. **R**, BMNH.M35721. **S**, HZM.1.31332. **T**, BMNH.M45656. **U**, BSPG.1971 XXVI-3. **V**, BSPG.1969 VII-966. **W**, BSPG.1968 VII-967, holotype of *V. ulmensis*. **X**, BSPG.1968 VII-968. **Y**, BSPG.1972 XVIII-1. **Z**, BMNH.M45654, holotype of *V. smithorum*. **AA**, HZM.6.21893. **AB**, BMNH.M35736. **AC**, BMNH.M35741. **AD**, BMNH.M35748. **AE**, HZM.3.30624. **AF**, BMNH.M35425. **AG**, HZM.8.36025. **AH**, BMNH.M51536. Teeth are from the left side except **A**, **D**, **E3**–**4**, **F1**–**3**, **I**–**K**, **M**–**N**, **P**, **W**, **Z2**, **AC**, **AE**–**AH**, which are right teeth reversed. The long scale bar is for *V. quaylei*, the short one for the rest. **Abbreviations**: **if**, interstitial facet.

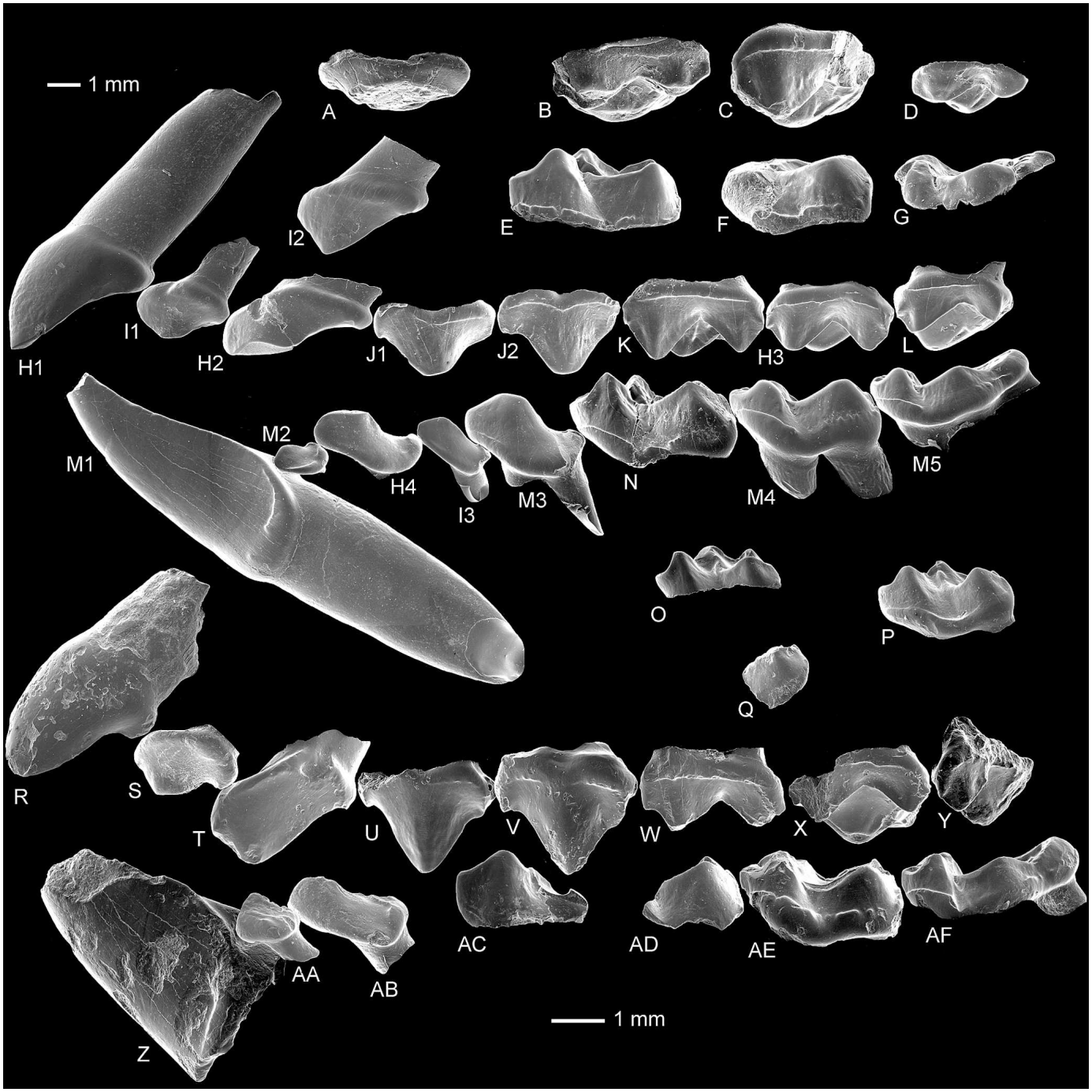


FIGURE 2. Scanning electron micrographs of gold palladium-coated epoxy casts of teeth of *Vectipithex* in buccal view, shown as from left side and reconstructed in approximate original position and orientation in the jaws. **A**–**G**, **P**, *V. ulmensis*. **H**–**O**, *V. smithorum*. **Q**–**AF**, *V. quaylei*. Teeth are: I1 (**H1**, **R**), I2 (**I1**, **S**), C (**H2**, **I2**, **T**), P3 (**A**, **J1**, **U**), P4 (**J2**, **V**), M1 (**B**, **K**, **W**), M2 (**C**, **H3**, **X**), M3 (**D**, **L**, **Y**), i1 (**M1**, **Z**), i2 (**M2**, **AA**), c (**H4**, **AB**), p3 (**I3**), p4 (**M3**, **AC**), m1 (**E**, **N**, **AD**), m2 (**F**, **M4**, **AE**), m3 (**G**, **M5**, **AF**), dp4 (**O**–**Q**). **A**, BSPG.1971 XXIV-4. **B**, BSPG.1971 XXIV-1. **C**, BSPG.1968 VII-1019. **D**, BSPG.1971 XXVI-1. **E**, BSPG.1968 VII-967, holotype of *V. ulmensis*. **F**, BSPG.1968 VII-968. **G**, BSPG.1972 XVIII-1. **H**, BMNH.M52036. **I**, BMNH.M45657. **J**, SMNS.42450. **K**, HZM.4.19545. **L**, HZM.25.29435. **M**, BMNH.M45654, holotype of *V. smithorum*. **N**, HZM.6.21893. **O**, BMNH.M45656. **P**, BSPG.1971 XXVI-3. **Q**, HZM.1.31332. **R**, HZM.4.31107. **S**, HZM.13.36684. **T**, BMNH.M36216. **U**, HZM.21.37620. **V**, BMNH.M35760. **W**, HZM.17.36927. **X**, BMNH.M37145, holotype of *V. quaylei*. **Y**, BMNH.M35721. **Z**, BMNH.M35736. **AA**, BMNH.M35741. **AB**, BMNH.M35748. **AC**, HZM.3.30624. **AD**, BMNH.M35425. **AE**, HZM.8.36025. **AF**, BMNH.M51536. Teeth are from the left side except **A**, **D**, **E**, **H2**–**4**, **I1**–**3**, **L**, **M2**, **R**–**S**, **U**–**V**, **AA**, **AC**–**AF**, which are right teeth reversed. The long scale bar is for *V. quaylei*, the short one for the rest.

the root. It suggests an oblique orientation of this tooth with respect to both I1 and the upper canine.

**Upper Canine**—This is similar in broad shape to I2, but relatively longer, more than twice as long as wide (Fig. 1F2). It is significantly longer than in *V. raabi* and other microchoerine genera. The lingual margin has a slight concavity midway along its length, where the weak lingual cingulum is interrupted (Fig. 3I3, L1). The main cusp is more mesial than in

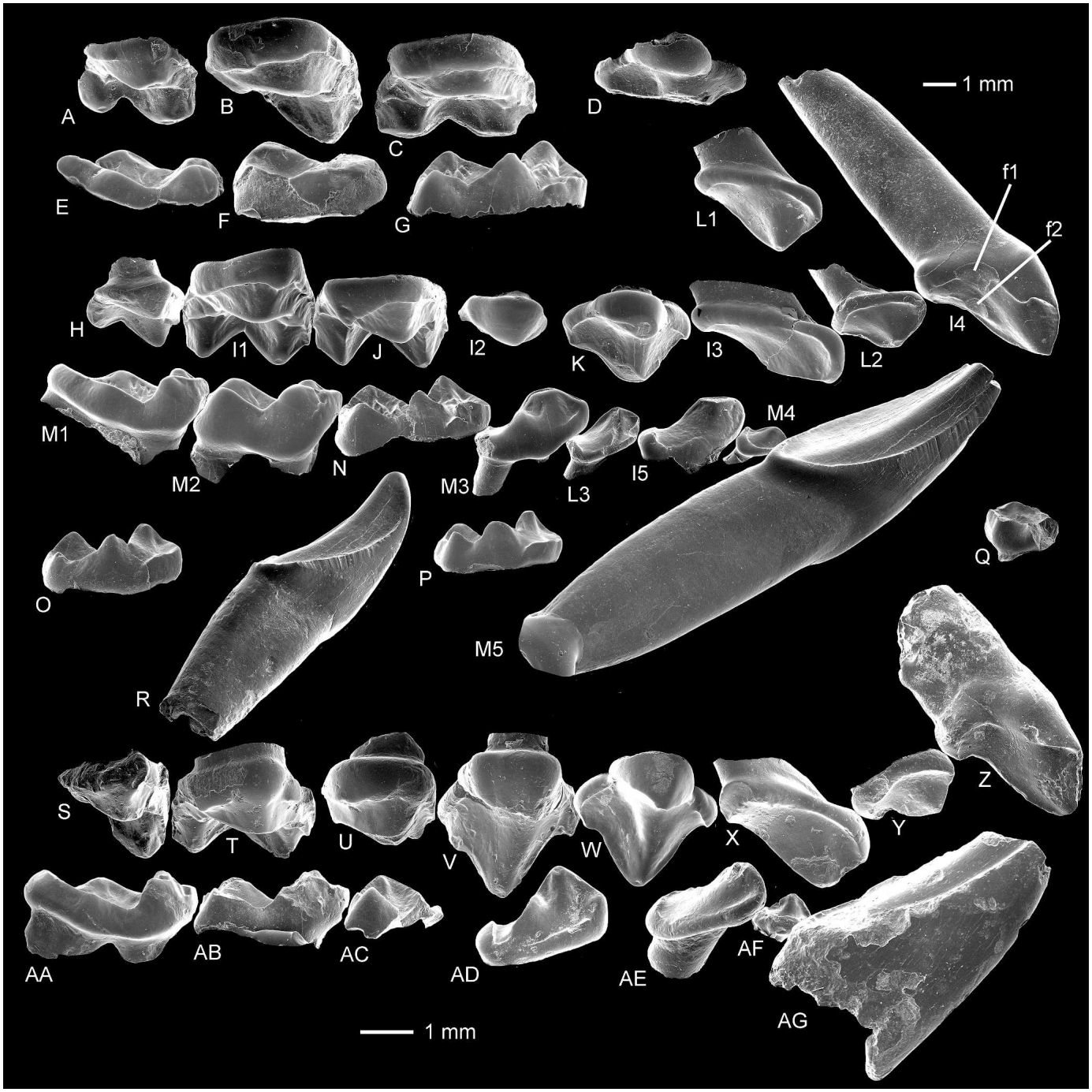


FIGURE 3. Scanning electron micrographs of gold palladium-coated epoxy casts of teeth of *Vectipithex* and *Microchoerus* in lingual view, shown as from left side and reconstructed in approximate original position and orientation in the jaws. **A**–**G**, **O**, *V. ulmensis*. **H**–**N**, **P**, *V. smithorum*. **Q**, **S**–**AG**, *V. quaylei*. **R**, *Microchoerus erinaceus*. Teeth are: I1 (**I4**, **Z**), I2 (**L2**, **Y**), C (**I3**, **L1**, **X**), P3 (**D**, **K**, **W**), P4 (**I2**, **V**), M1 (**C**, **J**, **U**), M2 (**B**, **I1**, **T**), M3 (**A**, **H**, **S**), i1 (**M5**, **R**, **AG**), i2 (**M4**, **AF**), c (**I5**, **AE**), p3 (**L3**), p4 (**M3**, **AD**), m1 (**G**, **N**, **AC**), m2 (**F**, **M2**, **AB**), m3 (**E**, **M1**, **AA**), dp4 (**O**–**Q**). **A**, BSPG.1971 XXVI-1. **B**, BSPG.1968 VII-1019. **C**, BSPG.1971 XXIV-1. **D**, BSPG.1971 XXIV-4. **E**, BSPG.1972 XVIII-1. **F**, BSPG.1968 VII-968. **G**, BSPG.1968 VII-967, holotype of *V. ulmensis*. **H**, BMNH.M53211. **I**, BMNH.M52036. **J**, HZM.4.19545. **K**, SMNS.42450. **L**, BMNH.M45657. **M**, BMNH.M45654, holotype of *V. smithorum*. **N**, HZM.6.21893. **O**, BSPG.1971 XXVI-3. **P**, BMNH.M45656. **Q**, HZM.1.31332. **R**, BMNH.M34834. **S**, BMNH.M35721. **T**, BMNH.M37145, holotype of *V. quaylei*. **U**, BMNH.M37692. **V**, BMNH.M35760. **W**, HZM.21.37620. **X**, BMNH.M36216. **Y**, HZM.13.36684. **Z**, HZM.4.31107. **AA**, BMNH.M51536. **AB**, HZM.8.36025. **AC**, BMNH.M35425. **AD**, HZM.3.30624. **AE**, BMNH.M35748. **AF**, BMNH.M35741. **AG**, BMNH.M35736. Teeth are from the left side except **A**, **D**, **G**, **I3**, **I5**, **L1**–**3**, **M4**, **R**, **U**–**W**, **Y**–**Z**, **AA**–**AD**, **AF**, which are right teeth reversed. The long scale bar is for *V. quaylei*, the short one for the rest. **Abbreviations**: **f1**, **f2**, facets 1 and 2, see text.

I2, making the occlusal outline in buccal or lingual view more canted and with a less obtuse angle between mesial and distal crests. The main cusp has a lingual convexity, whose axis dips slightly distally to the crown base. The single root has a mesiodistally elongate cross-section and extends much further mesially than in I2 (Fig. 2H2, I2). The mesial interstitial facet is mesiobasal in position, indicating that the upper canine lies at an angle to I2, tilted occlusally at its mesial end. The dis-

tal interstitial facet is indistinct, but appears to be essentially distal.

**P3**—In the absence of evidence for a P2, P3 is judged to have followed the upper canine. The single complete specimen is fairly worn and has an equilateral triangular outline (Fig. 1G1). The paracone is central along a mesiodistal axis and has a straight mesial crest and a slightly more prominent buccally concave distal crest. The lingual expression of the paracone is a bluntly angled convexity that trends towards but does not meet the protocone. The protocone is small and nearly central, very slightly mesial of a buccolingual axis passing through the paracone (Fig. 3K). It spawns cingula mesiobuccally and distobuccally. The former leading to the parastyle is weak and interrupted. The latter is stronger leading uninterrupted to the metastyle, originating more lingually and forming a slight distal bulge in the outline behind the protocone. The protocone lobe is very slightly constricted from the rest of the tooth. There is a weak buccal cingulum, isolated from the parastyle and metastyle (Fig. 2J1). There is no clear mesial interstitial facet, but the nature of the mesial margin of the parastyle, which is likely to have made contact with the tooth in front, does not suggest an overhang. The distal interstitial facet marks a shallow concavity in the distal metastyle wall for reception of the P4 parastyle.

**P4**—The only available specimens are two buccal fragments, one possibly belonging to the same individual as the P3, and two associated non-fitting fragments: part of the paracone and the protocone lobe. Buccally, the tooth is very similar to P3. The paracone and its crests are apparently taller, although the tooth is less worn than the P3 (Fig. 2J2). The parastyle is larger and more salient mesially (Fig. 1G2). The paracone is sharply angled lingually, unlike on P3 and slightly more mesially positioned. The protocone lobe of the other specimen (Figs. 1-E2, 3-I2) is very similar to that of *V. quaylei*, except that the lingual margin is slightly retracted distally and bears a vague hypocone-like swelling.

**M1–2**—Structure is essentially tribosphenic, but with a small cingular hypocone (Fig. 1E3, H). This is usually larger on M1 than on M2 and is not connected by a crest to the trigon. Of seven M1s and three M2s, only one, an M1, has a *Nannopithex* fold (postprotocingulum). There are distinct paraconule and metaconule, with their respective crests, situated midway between the protocone on the one hand and the paracone and metacone on the other. One M2 has a weak postmetaconule crista. The centrocrista is slightly concave buccally. The paracone and metacone are widely spaced and the parastyle is very small. The trigon basin is broadly U-shaped. A more or less continuous cingulum encircles the teeth (Figs. 2K, H3; 3I1, J). Sometimes an incipient pericone is developed on the lingual cingulum at the mesiolingual corner on M2 (Fig. 1E3). M1s are trapeziform or trapezoidal in outline, wider than long (see Table 1). The mesiobuccal corner forms a right angle and whether the lingual edge is parallel to the buccal edge or not depends on whether the hypocone is exactly distolingual or slightly more buccally situated. The short postmetacrista is oriented more distally than buccally. M2s are trapezoidal in outline, the mesiobuccal angle being 90 degrees or slightly less. The hypocone is no more than a crestiform shelf and situated buccal of the lingual margin, in some cases making the mesiobuccal angle acute. The postmetacrista is very short and nearly mesiodistally oriented.

**M3**—The three good specimens vary in size. Outline shape is almost D-shaped, the near straight side being mesial (Fig. 1I). The curve of the D is modified by the metacone, which bulges distobuccally. The metacone has an angled distobuccal edge, but no postmetacrista. There is a *Nannopithex* fold and no hypocone. The cingulum is interrupted around the protocone and metacone (Figs. 2L, 3H). The paraconule and metaconule bear crests as on M1–2, but these cusps are situated closer to the paracone and metacone than to the protocone. The protocone is sharply angled mesiolingually. Where unworn, the trigon basin enamel is faintly wrinkled.

**i1**—The crown is lanceolate and narrow mediolaterally (Fig. 1Z1). It recurves slightly apically. There is a short distobuccal cingulum that recurves apically at the distal end (Fig. 2M1). It creates a shallow concavity immediately apicad. As on I1, the buccal face curves around from the lateral to the anterior side, but the mesial surfaces of the two i1s meet at the midline. The mesial interstitial facet is marked by striations (Fig. 3M5) attributed to fur grooming (Rose et al., 1981). Comparison of the orientation of these striations with that of *Microchoerus* (Fig. 3R), where orientation of i1 is known from jaws (e.g., Wood, 1846, pl. 2, fig. 3b), indicates that i1 in *V. smithorum* was significantly procumbent, angled at about 30 degrees to the horizontal. The main cusp forms a gentle fold lingually from base to apex of the crown and is nearly paralleled anteriad by a cingulum. This cingulum descends basally from the mesial side of the apex, curving gradually distally posterior of the mesial interstitial facet to a low point posteriorly, then rising sharply to meet the base of the distal crest. In the triangle caused by apical confluence of the buccal and lingual cingula, lies the interstitial facet indicating contact with i2.

**i2**—This is tiny, procumbent, and heart-shaped in outline, the point facing mesially (Fig. 1Z2). The single cusp is very low (Figs. 2M2, 3M4) and crested mesially and distally, and its side walls are concave. The tooth is encircled by a cingulum. The mesial interstitial facet is mesiobasal and thus the tooth would have sat tilted against the back of the procumbent i1 as in *V. raabi* (e.g. Thalmann 1994, pl.2, figs. b, c). The distal interstitial facet is vertical on the distal wall, which bears a small stylar cusp.

**Lower Canine**—Outline is essentially asymmetrically D-shaped, the straight side lingual, the convex side buccal and distal (Fig. 1E4). The buccal part is less curved than the distal part. There is a single main cusp situated about a third of the distance from the mesial end. It has a prominent mesial crest and a short distal crest. The tooth is low crowned, procumbent, and elongate in buccal or lingual view (Figs. 2H4, 3I5). A weak lingual cingulum is interrupted in the middle. Distally, it joins a prominent distal cingular shelf, which extends a short distance buccally. The single root originates from the distal half of the tooth and its cross section is slightly elongate mesiobuccally-distolingually. The mesial interstitial facet is basal under the overhanging mesial lobe, aligned with the crown base. The distal interstitial facet is more disto-occlusally oriented but is only faintly visible on one specimen. This implies an oblique canted orientation for the lower canine and that it was also overhung slightly by p3.

**p3**—This is similar in shape to the lower canine, but smaller and less elongate (Fig. 1F3). It is, however, more triangular than D-shaped in outline, the distal edge being essentially transverse, and the buccal and lingual sides gently curved, converging on the mesial apex. There is a complete lingual cingulum and a faint incomplete buccal cingulum (Figs. 2I3, 3L3). The mesial interstitial facet is mesiobasal and the distal interstitial facet is disto-occlusal, supporting overlap on the lower canine and by p4. The single root is slightly elongate buccolingually in cross section.

**p4**—Despite wear, both specimens were clearly originally low crowned and procumbent. The lingual basal crown margin is angled up mesial of the metaconid (Fig. 3M3). The mesiodistally oriented paracristid lacks a paraconid (Fig. 1Z3). The metaconid is cuspate in one specimen, crestiform in the other. The very shallow poorly developed talonid basin is open lingually. Cingula are weak and restricted to the mesial parts of the buccal and lingual walls. Two roots arise from the distal two thirds of the crown base (Fig. 2M3). The mesial interstitial facet is basal as on the lower canine and implies slightly oblique orientation and significant overhang of the much smaller p3. The distal intersti-

tial facet is also oriented as on p3 and lower canine, and indicates overlap by m1.

**m1**—Outline is bullet-shaped, reflecting the combination of protoconid, metaconid, hypoconid, and entoconid, with mesially protruding open trigonid (Fig. 1AA). There is no paraconid, but simply a paracristid that recurves distally as a strong cingulum, weakly cuspate in two specimens, from the mesial extremity along the lingual margin nearly as far as the metaconid, partly enclosing the trigonid basin. The openness of the trigonid is emphasized by the lingual protoconid rib merging basally with the metaconid in three of five specimens. One unworn specimen has enamel wrinkling in both the trigonid and talonid basins (Fig. 1AA). The entoconid is slightly lower than the hypoconid (Fig. 3N) as is usual in microchoerines (except *Pseudoloris* and '*Nannopithex*' *humilidens*), but what is unusual is that the metaconid is much lower than the protoconid. In the unworn HZM.6.21893, it is not much more than half its height. The cristid obliqua is gently convex buccally and approaches the trigonid midway between the protoconid and metaconid, joining it only at the base. The hypoconulid is marked by little more than a bend in the postcristid where a distal salient descends to a postcingulid. An ectocingulid extends a variable distance distally along the buccal margin but is always interrupted at the hypoconid (Fig. 2N). Cresting is well marked all around the talonid basin, the postmetacristid and pre-entocristid being nearly as strong as the postcristid. The mesial interstitial facet is mesiobasal, confirming the slight overhang of this tooth on p4. The distal interstitial facet is nearly vertical, showing no overlap by m2.

**m2**—The two specimens show a similar pattern of cusps, crests, and cingula to m1, but with a shorter trigonid and more or less parallel buccal and lingual margins, giving a near rectangular outline (Fig. 1Z4). The difference in height between the protoconid and metaconid is also less marked. There is a weak paraconid and cuspate lingual trigonid cingulum (Figs. 1Z4, 3M2). These attain more prominence because of the shortness and erect stance of the trigonid (Fig. 2M4). The straight cristid obliqua joins the trigonid at a more buccal position below the tip of the protoconid. The protoconid is joined by a crest to the mesial side of the metaconid. The talonid basin has wrinkled enamel.

**m3**—The shape of the trigonid (Figs. 2M5, 3M1) and orientation of the cristid obliqua are very similar to that of m2, except that the recurved paracristid joins the metaconid to enclose completely the trigonid basin (Fig. 1Z5). Distal of the trigonid, end-of-the-row tapering means that the talonid outline narrows, the entoconid weakens and the hypoconulid takes the usual form of a distally expanded lobe. In three specimens, the lobe is narrow, elongate, and tapering. In a fourth, it is short, broad, and blunt ended, the main hypoconulid cusp being positioned lingually very close to a distally shifted entoconid. All three show enamel wrinkling in the talonid basin. The mesial interstitial facet is vertical and shows that m3 abuts m2 with the mesial protrusion of the former fitting just lingual of the hypoconulid of the latter (demonstrable on the teeth of one individual).

**dp4**—Wear is light but the buccal side is damaged basally (Fig. 2O). The crown is low with a procumbent very open trigonid (Fig. 1T). The metaconid is set far distally and the protocristid is notched (Fig. 3P). The entoconid is nearly as tall as the hypoconid and the hypoconulid is close to the hypoconid.

## Discussion

Although teeth are isolated, four groups of teeth (those listed as "associated" above under holotype and paratypes) were found closely associated in their sediment sample. This evidence, together with similar wear states, non-repetition of elements, and matching interstitial facets (e.g., Fig.1Z1) strongly suggests that the associations represent individuals. This supports our interpretation that the material represents a single species (see also Occlusion section below). These dental associations are recorded from three stratigraphic levels: the How Ledge Limestone, the Hatherwood Limestone Member, and the Bembridge Limestone Formation. Associated teeth in Figures 1–3 are indicated by sharing the same letter with different number suffixes.

### *VECTIPITHEX ULMENSIS* (Schmidt-Kittler, 1971) comb. nov.
(Figs. 1A–D, U, W–Y; 2A–G, P; 3A–G, O)

v* 1971 *Adapis ulmensis* Schmidt-Kittler:177–181, figs. 10–11, pl. 13, fig. 11.
v non 1971 *Adapis ulmensis* Schmidt-Kittler:179–180, fig. 12.
v. 1977 *Protoadapis ulmensis* (Schmidt-Kittler): Schmidt-Kittler: 182–185, figs. 1–5.
v. 1977 Adapidae sp.: Schmidt-Kittler:185–186, figs. 6–7.

**Holotype**—Right m1 (BSPG.1968 VII 967) from the Priabonian (MP19 Headonian ELMA) fissure filling of Ehrenstein 1, Bavaria, Germany.

**Paratypes**—Left m2 (BSPG.1968 VII 968) and a lower cheek tooth fragment (BSPG.1969 VII 966) that does not belong to *V. ulmensis*, from Ehrenstein 1.

**Referred Specimens**—Right P3 (BSPG.1971 XXIV-4), left M1 (BSPG.1971 XXIV-1), right M2 lacking distobuccal corner (BSPG.1971 XXIV-3) from Ehrenstein 3; left M2 (BSPG.1968 VII-1019) from Ehrenstein 1; left m3 (BSPG.1972 XVIII-1) from Herrlingen 3; right M3 (BSPG.1971 XXVI-1), left dp4 (BSPG.1971 XXVI-3) from Ehrenstein 2; all Bavaria, Germany.

**Emended Diagnosis**—Largest species of *Vectipithex*, M1 length: 4.11 mm. m1 length: 4.63 mm. Length of M1 is 83% of width; length of m1 150% of width. P3 with protocone nearly subsumed by lingual crests (Figs. 1A, 2A, 3D). Upper molars with rounded lingual profile and lower molars with prominent postmetacristid, m2–3 with sloping distal wall (Figs. 1X, Y; 2F, G; 3E, F). (Incisors, canines, P4, and lower premolars unknown). *Vectipithex smithorum* is slightly smaller and other species of the genus much smaller. All other species have lesser length/width proportions of molars, more distinct P3 protocone, more angular upper molar lingual profile, weaker lower molar postmetacristids, and vertical distal wall of m2–3 trigonid. *V. raabi* has M1–2 *Nannopithex* fold. *V. quaylei* has M2 with *Nannopithex* fold.

## Discussion

The type and referred material listed above has been fully described by Schmidt-Kittler (1971, 1977). However, in the light of *V. smithorum*, which closely resembles *V. ulmensis*, some of the *V. ulmensis* teeth can be reidentified as to locus and those previously identified as 'Adapidae sp.' can be reassigned to this species.

The more complete paratype tooth was originally identified as p4 (Schmidt-Kittler 1971, fig.11; herein Fig. 1-X) and its molariform structure fitted identification with the genus *Adapis*. It was later (Schmidt-Kittler 1977: 184) reidentified as m1/2. Size and structure are similar to the holotype m1 especially in the orientation of the cristid obliqua (Fig. 1-W). It differs, however, in having a more erect trigonid, which, despite heavy tip wear and postmortem abrasion, shows taller paracristid and associated minor cusps as on m2 of *V. quaylei*, and is identified to this locus (Figs. 2-E–F, 3-F–G). Indeed it is closer morphologically to *V. quaylei* than to *V. smithorum*, which has a shorter trigonid and less developed postmetacristid.

The other paratype is a talonid fragment identified originally as p3 (Schmidt-Kittler 1971, fig.12; herein Fig. 1V). It was later re-identified as p4 (Schmidt-Kittler 1977: 184). However, it cannot be identified with any of the loci of *V. smithorum*. It is therefore not a p3 or a p4 of *V. ulmensis*. It looks most like a p4 of an adapine, the obliquity of the cristid obliqua suggesting

*Leptadapis*. It is too small for *L. magnus*, which is recorded from the site (Schmidt-Kittler 1971), and may belong to the smaller *Leptadapis assolicus* Richard, 1940.

Two referred damaged teeth identified originally as M3 (Schmidt-Kittler 1977, figs. 1, 2) can be re-identified by comparison with *V. smithorum* as M2 (Figs. 1C; 2C; 3B). Although incomplete, their outline appears to taper distally slightly. Another upper molar identified originally as M1/2 resembles M1s of *V. smithorum* in its acute distobuccal corner with distobuccally oriented postmetacrista, and is so re-identified (Figs. 1B; 2B; 3C).

The M3 (Figs. 1D; 2D; 3A) identified as 'Adapidae sp.' (Schmidt-Kittler 1977, fig.7) can therefore be reidentified as belonging to *V. ulmensis*, as the M3s previously identified to this tooth locus have been reassigned to M2. The m1 attributed originally to 'Adapidae sp.' (Schmidt-Kittler 1977, fig. 6) is here reidentified as dp4 of *V. ulmensis* (Figs. 1U, 2P, 3O). It is unworn but very similar to the same tooth of *V. smithorum*, differing mainly in having a smaller, more distobuccally positioned entoconid, and less buccally situated hypoconulid.

*VECTIPITHEX QUAYLEI* (Hooker, 1986) comb. nov.
(Figs. 1J–S, AB–AH; 2Q–AF; 3Q; S–AG)

vp* 1986 *Nannopithex quaylei* Hooker:249–251, 254–255, pl. 4, figs. 9–13, pl. 5, figs. 1, 5a–c, pl. 6, figs. 1a–c.
v non 1986 *Nannopithex quaylei* Hooker: pl. 4, fig. 14.
vp 1986 *Nannopithex* sp. 1: Hooker:250–251, 254, pl. 4, figs. 1, 5, 8.
v. 1986 Adapinae indet.: Hooker:280, 282, pl. 11, fig. 7.
v. 1994 *Nannopithex quailey* [sic] Hooker: Thalmann:102, 104–107.
v. 2002 *Nannopithex quaylei* Hooker: Gunnell and Rose:49–50.
v. 2005 *Nannopithex quaylei* Hooker: Hooker et al.:90–93, fig. 3.10h.

**Holotype**—Left M2 (BMNH.M37145), from the Creechbarrow Limestone Formation (Bartonian), Creechbarrow, Dorset, UK (see Hooker 1986 for stratigraphy).

**Paratypes**—Left I1 (BMNH.M37154), right I1 (BMNH.M35434), left P4 (BMNH.M35759), two right P4s (BMNH.M35760, M37144), left M3 (BMNH.M35721), left i1 (BMNH.M35736), left c (BMNH.M35748), left m1 talonid (BMNH.M35720), right m1 talonid (BMNH.M35425), and a left m3 talonid (BMNH.M37147) here re-identified to a different taxon; all from the same horizon and locality as the holotype.

**Referred Specimens**—Left I1 (HZM.5.31509), two right I1s (HZM.4.31107, 12.36626), left I2 (HZM.2.34374), two right I2s (BMNH.M35218, HZM.13.36684), left C (BMNH.M36216), two right P3s (HZM.21.37620, 20.37738), left P4 buccal half (HZM.1.30588), left M1 buccal half (HZM.17.36927), right M1 lingual half (BMNH.M37692), left M2 lingual half (HZM.9.36264), right M2 lingual half (HZM.14.36803), left M3 lingual half (BMNH.M35722), right M3 lingual half (HZM.18.36948), right i2 (BMNH.M35741), right p4 (HZM.3.30624), right m2 (HZM.8.36025), left m2 talonid (HZM.10.36342), two left m3s (BMNH.M35427, M37153), right m3 (BMNH.M51536), four left m3 trigonids (BMNH.M35215, M37152, HZM.7.35426, 16.36908), two right m3 trigonids (BMNH.M36214, HZM.2.34462), left m3 talonid (HZM.5.35213), right m3 talonid (BMNH.M35727), left dp4 talonid (HZM.1.31332), right dp4? trigonid fragment (BMNH.M45653); all from the same horizon and locality as the holotype.

**Emended Diagnosis**—Medium-sized *Vectipithex*, M2 length: 2.69 mm. m2 length: 3.06 mm. M1 without and M2 with *Nannopithex* fold. M1–2 postmetacrista distobuccally oriented. (p3 and m1 trigonid unknown). The other species have M1–2 postmetacrista nearly mesiodistally oriented. *V. smithorum* and *V. ulmensis* are larger, with M1–2 with greater length-width proportions and lacking M2 *Nannopithex* fold. *V. raabi* is smaller and has M1 with *Nannopithex* fold.

**Description**

The original composition of the taxon is modified here by inclusion of some tooth loci that were originally included in *Nannopithex* sp. 1, a smaller microchoerine distinct from *Vectipithex quaylei*. Some doubt was expressed as to whether the m3s attributed to *N.* sp. 1 (e.g., Hooker 1986, pl. 4, fig. 8; herein Figs. 1-AH, 2-AF, 3-AA) belonged to this species or to '*N.*' *quaylei* (Hooker 1986:251). Size comparisons with *V. smithorum* indicate that these four m3s should be referred to *V. quaylei*. The paratype m3 (Hooker 1986, pl. 4, fig. 14) is re-identified as the apatemyid *Heterohyus morinionensis* Hooker, 1986, on the basis of a very shallow talonid basin, crestiform entoconid, low hypoconid and bulbous hypoconulid. The M3 lingual half attributed to *N.* sp. 1 (Hooker 1986, pl. 4, fig. 5) is transferred to *V. quaylei*. The tooth identified as I2 of *N.* sp. 1 (Hooker 1986, pl. 4, fig. 1) is here reidentified as i2 of *V. quaylei*. The lower canine was originally identified as p3 (Hooker 1986, pl. 4, fig. 12).

These actions leave *N.* sp. 1 represented by I1 and m1 that are completely known, plus fragments of P3 and M2. Most of the similarities to *V. quaylei* concern primitive characters, a number of which are to be found also in *N. zuccolae*. The presence of a protocone-paracone crest and lack of a parastyle on the P3 fragments is more like *Nannopithex filholi* (Chantre and Gaillard, 1897) than any species of *Vectipithex*. '*N.*' sp. 1 will remain indeterminate until more, better preserved teeth can be found. Below, the *V. quaylei* material is redescribed in light of knowledge of *V. smithorum*.

**I1**—This is broadly similar in shape to that of *V. smithorum*, but is relatively slightly taller, base to apex, so that the curvature of the anterior margin towards the cusp tip is less (Fig. 2R). It has a deeper medial concavity in the outline, which means a more distinct valley between the main cusp and the heel (Fig. 1J). The medial cingulum curves gently basally, rather than stepping suddenly, and dies out at the medial concavity (Fig. 3Z). The crown base is perpendicular to the long axis of the crown buccally. The distal interstitial facet is oriented as on *V. smithorum* and there is no observable mesial interstitial facet, indicating likewise a gap between the two upper first incisors.

**I2**—Morphology is identical to *V. smithorum* (Figs. 1K, 2S, 3Y), but size is smaller. The mesial interstitial facet, visible on two of the teeth, is mesiobasal, supporting its postulated position in *V. smithorum*.

**Upper Canine**—The proportions are elongate as in *V. smithorum*, but in contrast there is a complete lingual cingulum and near complete buccal cingulum, which dies out only as the mesial end is approached (Figs. 1L, 2T, 3X).

**P3**—HZM.21.31620 closely resembles P3 in *V. smithorum*, although with a more waisted protocone lobe (Figs. 1M, 2U, 3W). HZM.20.37738 differs in being more transversely elongate, with a lingually more extensive protocone lobe, with more mesially placed protocone, reminiscent of P4. It has a slightly taller parastyle and metastyle, also approaching the structure of P4. Both teeth, however, have the parastyle mesially protruding, unlike P4, and this forms the main criterion for identifying both teeth as P3.

**P4**—This is significantly more transversely elongate than the more P4-like of the P3s. Its protocone lobe is less tapering lingually and it is not waisted (Fig. 1N). The parastyle, paracone, postparacrista and metastyle are all taller and the postprotocrista is stronger, curving around a more angled distolingual tooth margin delimited buccally by a vertical groove (Figs. 2V, 3V). The only discernable difference from the incompletely known *V. smithorum* P4 is a slightly more angled postparacrista, which is consistent for the four *V. quaylei* specimens known.

**M1**—This is represented by a lingual half fragment, originally identified as an adapine (Hooker 1986, pl. 11, fig. 7; herein Figs. 1P, 3U), and a buccal half fragment (Figs. 1O, 2W). The former is reidentified here on the basis of morphological similarity to M1 of *V. smithorum*. There is a small hypocone and the lingual border of the tooth appears mesiodistally oriented (Figs. 1P, 3U). There is no *Nannopithex* fold, although a faint crest joins the hypocone to the postprotocrista. A cingulum as preserved is nearly complete except around the protocone, where spot penetration of dentine suggests the former presence of a small pericone. The buccal half shows the autapomorphic distobuccal orientation of the postmetacrista (Fig. 1O).

**M2**—The holotype is relatively slightly shorter mesiodistally than those of *V. smithorum*. All three specimens also differ morphologically in having a distinct *Nannopithex* fold (Figs. 1Q, 2X), although it is weak in one. They also differ from *V. smithorum* in having a major interruption to the cingulum around the protocone (Fig. 3T). The holotype is recognisable as M2 because of its very short, near mesiodistally oriented postmetacrista and acute lingual angle caused by the relatively buccal position of the hypocone shelf. The other specimens share with it the same lingual structure.

**M3**—No specimen is complete, one (BMNH.M35721) being poorly preserved, lacking the distobuccal corner (Figs. 1R, 2Y, 3S), the others (including BMNH.M35722, originally referred to *Nannopithex* sp. 1, Hooker 1986, pl. 4, fig. 5) being only lingual halves. Although outline shape cannot be determined, they differ from *V. smithorum* in having an acute lingual margin made more pronounced in two cases by a prominent pericone. Moreover, M35721 has a protocone whose lingual wall is carinate. Lingual outline is therefore more like *V. raabi* than *V. smithorum*. All have a *Nannopithex* fold.

**i1**—The single specimen is broken apically and anterobasally (Figs. 1AB, 2Z). What remains is very similar morphologically to *V. smithorum*. The only observable differences are that the buccal cingulum extends further anteriorly and the mesial surface, bordered by the mesial cingulum, is more extensive mesiodistally, and so the lingual rib is correspondingly more distal in position, making the distal wall more transverse (Fig. 3AG). In the extent of its mesial surface, *V. quaylei* is like *V. raabi*, but here the similarity ceases. *Vectipithex raabi*, unlike either *V. quaylei* or *V. smithorum* has a rib that dies out half way down the crown and has a deeper exodaenodont buccal lobe.

**i2**—This is slightly shorter, but significantly narrower than in *V. smithorum* (Fig. 1AC). In comparison, it is irregularly oval in outline, has a narrower buccal cingulum (Fig. 2AA), but a wider shelf-like lingual cingulum and the main cusp forms a rib lingually (Fig. 3AF).

**Lower Canine**—This is nearly identical morphologically to that of *V. smithorum* (Figs. 1AD, 2AB, 3AE). The only observable difference is that the main cusp is situated a little further mesially, as in *V. raabi*, making the slope of the mesial crest steeper.

**p4**—The single tooth is broken distobuccally (Fig. 2AC). It has a crestiform metaconid (Fig. 1AE), like one of two specimens of *V. smithorum*. It differs from this species in having a lingually salient paracristid, a straight basal lingual crown margin, and a nearly continuous lingual cingulum (Fig. 3AD).

**m1**—Identification of left and right talonid fragments rests on the orientation of the cristid obliqua, which is buccally convex (Fig. 1AF) and is so oriented that it would join the trigonid approximately midway between the protoconid and metaconid (cf. m2). Both specimens are unworn and so similar that they may belong to the same individual. They are nearly identical in morphology (Figs. 2AD, 3AC) to the unworn m1 of *V. smithorum*, but differ in entirely lacking enamel wrinkling.

**m2**—The talonid of these teeth is very similar to that of *V. smithorum*, especially in the buccally situated cristid obliqua, also determining them as m2 (Figs. 1AG, 2AE, 3AB). The trigonid of the complete tooth is, however, relatively longer and more procumbent, the mesial interstitial facet having a slightly more basal orientation.

**m3**—The newly referred specimens include those originally attributed to *Nannopithex* sp. 1 from Creechbarrow (Hooker 1986). Referring to *V. smithorum*, their size and morphology can be seen to fit well with *V. quaylei.* Three essentially complete teeth plus six trigonid and two talonid fragments give a reasonable idea of variation. Most are relatively slightly more elongate than *V. smithorum* (Table 1) and some have a relatively longer trigonid (Figs. 1AH, 2AF, 3AA). In these respects, *V. quaylei* differs to a similar degree from *V. raabi*. In four specimens, enamel wrinkling is largely restricted to the hypoconulid lobe (e.g., Fig. 1AH; Hooker, 1986, pl. 4, fig.8), but in a fifth (BMNH.M35727) it fills the talonid basin. There is variation in the strength of the accessory cusp between the paraconid and metaconid and in the paraconid itself. In most, all three cusps are joined by a crest, but in two cases this is interrupted between the accessory cusp and paraconid. In two, the accessory cusp is crested buccally (Fig. 1AH). In general, the trigonid cusps are more prominent than in *V. smithorum*.

**dp4**—The talonid fragment is worn, but shows similar height and cusp arrangement to that of *V. smithorum*, only differing in having a slightly distally concave postentocristid (Figs. 1S, 2Q, 3Q). A doubtful trigonid fragment that consists of only the protoconid and paracristid and is broken basally resembles *V. smithorum* and *V. ulmensis*.

## Discussion

In many respects, *V. quaylei* is very similar morphologically to *V. smithorum*, being simply smaller. However, some features more closely resemble *V. raabi* and seem to be primitive. The unknown m1 trigonid inhibits comparisons with the other species. The generally small sample size may mean undersampling of the individual variation. The emended diagnosis selects the characters judged more likely to be constant, in light of observed individual variation.

### *VECTIPITHEX RAABI* (Heller, 1930) comb. nov.

v* 1930 *Necrolemur raabi* Heller:35–38, 41, pl. 5, figs. 5, 6.
v. 1994 *Nannopithex raabi* (Heller): Thalmann:26–30, figs. 2.1–2.2, pl. 3, figs. a–f.
v. 1994 *Nannopithex abderhaldeni* (Weigelt, 1933): Thalmann: 30–33, figs. 2.3–2.4, pl. 2, figs. a–e.
? 1994 *Nannopithex barnesi* Thalmann:34, fig. 2.5, pl. 2, figs. f–h. (N.B. For synonymies between 1930 and 1994, see Thalmann (1994)).

**Lectotype**—Right dentary with c, p3–m3 (GMH.CeI-4254) from the oberes Hauptmittel, Lutetian, Eocene of Cecilie Pit, Geiseltal, Germany.

**Paralectotype**—Right dentary with i1–2, canine, p4–m3 (GMH.CeI-4255) from the same horizon and locality as the lectotype.

**Referred Specimens**—Those listed by Thalmann (1994) for the species '*N*'. *raabi*, '*N*'. *abderhaldeni*, and tentatively '*N*.' *barnesi*.

**Emended Diagnosis**—small *Vectipithex*, mean M1 length: 2.11 mm; mean m1 length: 2.07 mm (Thalmann 1994). I2 and C relatively short. Cheek teeth relatively high-crowned. m1–2 with relatively short talonids with mesiobuccally oriented preentocristid. Upper canine mesiodistally short. P3 protocone mesiolingually placed and with strong postparacrista. M1–2 with *Nannopithex* fold. m1–2 paraconid strong and cuspate. All the other species are larger, have lower crowned cheek teeth, P3 with weaker postparacrista and more centrally positioned proto-

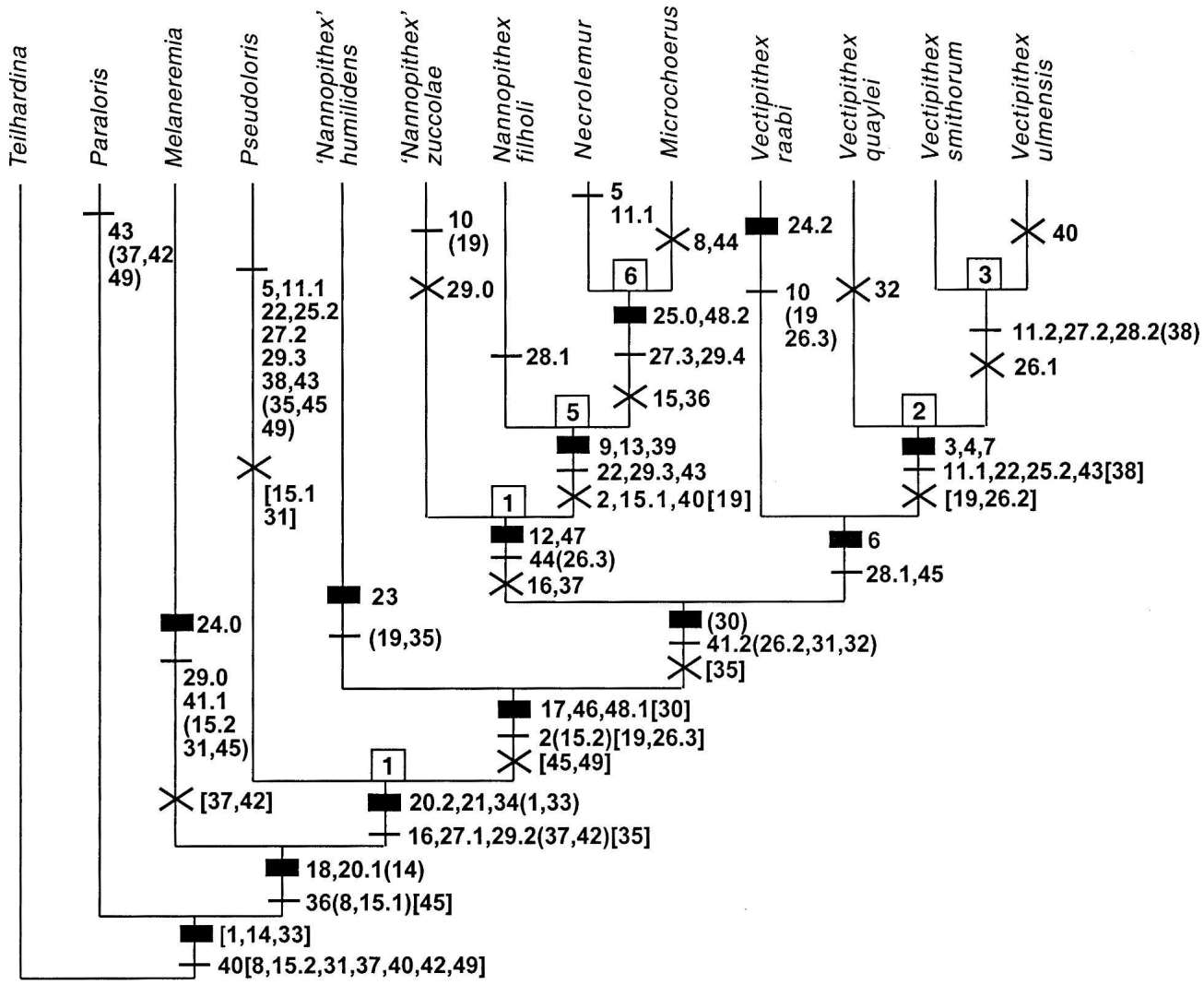


FIGURE 4. Maximum parsimony cladogram of Microchoerinae generated by PAUP 4.0 from the character-taxon matrix in Appendix 2, showing character-state changes; see Appendix 1 for explanation of numbered characters. Broad bar, synapomorphy; narrow bar, normal polarity homoplasy; X, reversal. Characters that vary with different optimizations are enclosed between () for Deltran and between [] for Acctran. The zero state is indicated only where it is not the primitive state (viz. characters 24, 25, and 29). Numbers in boxes at nodes are Bremer support indices (Bremer 1994).

cone, no M1 *Nannopithex* fold, reduced or crestiform paraconids on m1–2, and longer m1–2 talonids with longitudinal preentocristids. *Vectipithex ulmensis* and *V. smithorum* have longer upper molar proportions and no M2 *Nannopithex* fold. *Vectipithex quaylei* and *V. smithorum* have mesiodistally longer I2 and C.

**Occurrence**—Ober Mittelkohle to Oberkohle, Lutetian (MP13, Geiseltalian ELMA, doubtfully also MP14, Robiacian ELMA), Eocene, of Geiseltal, Germany.

## OCCLUSION

The different isolated tooth loci of *V. smithorum* have been reconstructed as upper and lower dentitions, with their spatial relationships and orientations based on position and orientation of interstitial facets and, in the case of canines and incisors, partly on orientations of the root. However, the orientation of i1 with respect to the very small i2 is less easy to judge precisely. Therefore, i1 has been oriented by aligning the fur-grooming scratches on its mesial interstitial facet with those of *Microchoerus erinaceus* (Fig. 3M5, R). This shows that i1 of *V. smithorum* was significantly procumbent, more so than *V. raabi* and substantially more so than *Microchoerus*, lying at 30 degrees to the horizontal. Reconstruction of the dentitions leaves no room for a P2, although the exact relative positions between upper and lower dentitions cannot be attained because several different individuals are involved (Figs. 2H–N, 3H–N). The upper and lower dentitions of *V. quaylei* have been reconstructed similarly to those of *V. smithorum*, although in the former species p3 is as yet unknown. The general pattern is very similar to that of *V. smithorum*, however, and it is judged that P2 was missing here too (Figs. 2R–AF, 3S–AG). In addition, no fur-grooming scratches could be detected on i1 of *V. quaylei*, so the orientation of this tooth could not be reconstructed accurately by this method.

Well-developed buccal and lingual phase facets are found on the molars as on other omomyids (Butler 1973). P4 has buccal phase facets, but wear on the only known protocone of this tooth is abrasive, there being no lingual phase facets preserved (Fig. 1G2, E2). P3 has buccal phase only, this being restricted to the distal part of the postparacrista, where it sheared against the p4 paracristid (Fig. 2J1, M3). Reduction of the P3 protocone reflects the reduction of p3, there being no basin for lingual phase. No

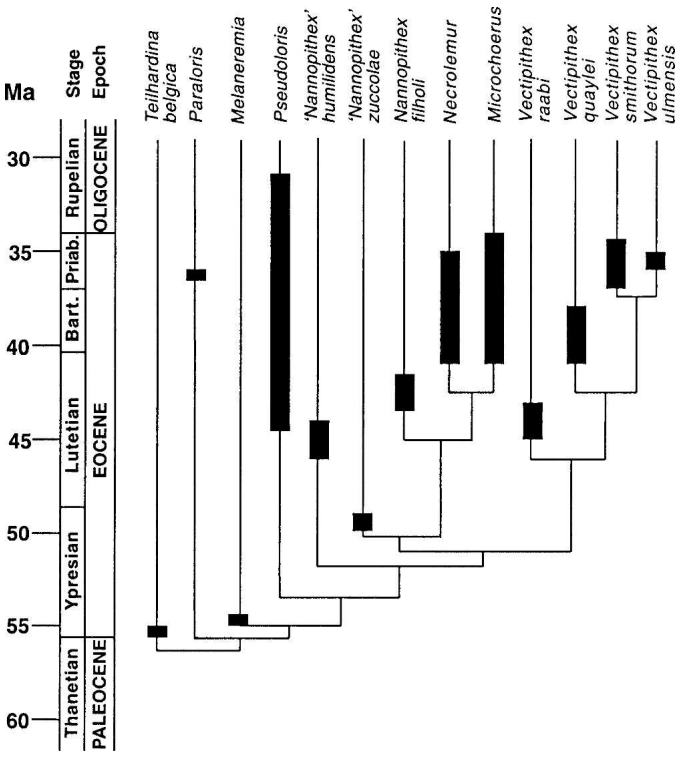


FIGURE 5. The maximum parsimony cladogram from Figure 4 fitted to the stratigraphy. Thickened sections of branches indicate stratigraphic range of taxon. Timescale follows Gradstein et al. (2004). Stratigraphic ranges are from Brunet et al. (1987), Fahlbusch (1995), Hooker (1986, 1992, 1996, 2007), Köhler and Moyà-Solà (1999), Remy et al. (1987), and Thalmann (1994). **Abbreviations**: **Bart**., Bartonian; **Priab**., Priabonian.

distinct wear facets have been observed on more mesial teeth, only abrasive wear. This has affected particularly cusp tips, which are often planed off, but also crests whose edges have become rounded and smooth (e.g. Figs. 1E4; 2H2,H4; 3I3,I5). Tip wear also affects the main cusps of the premolars and molars, indicating that puncture-crush was an important mode in the chewing cycle of *V. smithorum*. A very similar pattern of wear pertains for *V. quaylei* and for the few tooth loci known in *V. ulmensis*.

I1 of *V. smithorum* bears two patches of wear on its lingual surface, where dentine has been penetrated. They are labelled f1 and f2 (Fig. 3I4). Facet f1 is obliquely oriented and intersects the medial cingulum slightly posterior of its midpoint. Facet f2 is situated more laterally and also less basally because it is closer to the sharp posterior crest. It shows striations that are oriented approximately transversely. In view of the relative positions of the facets and the wear sense indicated on f2, it is likely that f2 was created during buccal phase, the incisor moving medially to anteromedially along with the other teeth. When full centric occlusion was reached, i1 came to rest more basally on the medial and mesial side of I1 producing f1. The i1 probably moved out of contact with I1 during lingual phase as no other facets are observable on I1. In *V. quaylei* (Fig. 3Z) and *V. raabi*, f2 is situated more basally relative to f1 than in *V. smithorum* if the teeth are oriented with their root axes parallel. This may be because there is a more pronounced concavity here in the former two species (Fig. 3Z). The fact that *V. raabi* has less procumbent i1 (lying at an angle of about 40 degrees to the horizontal: Thalmann 1994, pl.2, figs. b–c, pl.3, figs. c–d), and by implication I1, than in *V. smithorum* may mean that first incisor orientation in *V. quaylei* was steeper like that of *V. raabi* rather than *V. smithorum*.

Thalmann (1994: 77–82) showed that *V. raabi* has an unusual occlusion pattern of its premolars, canines, and incisors as seen in lateral view. Small sizes of i2 and p3 allowed larger upper canine and P3 to interlock with the lower teeth in a zigzag rather like the beak of a parrot (Thalmann 1994, fig.3.10). He interpreted the diet of *V. raabi* as including large objects including seeds and insects, which were thereby crushed as in a bird's beak. Both *V. quaylei* and *V. smithorum* have a similar interlocking pattern in lateral view (Fig. 2H1–J2, M1–M3), but it differs from *V. raabi* in being less pronounced probably because the anterior dentition is more extended anteriorly, the canines and lower premolars being more elongate and, in *V. smithorum*, the first incisors being more procumbent. *Vectipithex quaylei* and *V. smithorum* also have teeth that are lower crowned than *V. raabi* and the incidence of enamel wrinkling is variable, suggesting a softer diet. This together with larger size and much tip wear also suggests a greater proportion of fruits and seeds versus insects in the diet.

## PHYLOGENETIC ANALYSIS

To establish the phylogenetic relationships of the species of *Vectipithex* to one another and of the genus *Vectipithex* within the Microchoerinae, a cladistic analysis was undertaken using PAUP version 4.0b10 (Swofford 2000). The matrix consists of 13 taxa and 49 characters (see Appendices). On the basis of an analysis of primitive omomyids (Hooker 2007), *Teilhardina* was chosen as outgroup taxon. Most states were taken from *T. belgica* (Teilhard, 1927) and a few from *T. asiatica* Ni, Wang, Hu and Li, 2004 (see Appendix 1). Multistate characters were treated as ordered as they comprised transformation series. Using a Branch and Bound search, PAUP found one maximum parsimony cladogram of 105 steps, with a consistency index excluding uninformative characters of 0.5859 and a retention index of 0.6985 (Fig. 4).

Despite being the earliest member of the genus, *V. raabi* is derived in its elevated crown height and long P3 postmetacrista. Reversal to the primitive condition of the orientation of the M1–2 postmetacrista is the only autapomorphy of late Middle Eocene *V. quaylei*, which suggests that it is not directly ancestral to the two Late Eocene species. German *V. ulmensis* is overall more derived than its English contemporary *V. smithorum* (see diagnosis for additional autapomorphies), although it remains poorly known. '*Nannopithex*' *humilidens* has a mosaic of characters shared with other species of this paraphyletic genus and with *Pseudoloris*. Its upper dentition is unknown, but should this be found, its position as stem member of the *Vectipithex* and *Microchoerus*+*Necrolemur*+*N. filholi*+'*N*'. *zuccolae* clades may change. *Paraloris* is more distantly related to *Pseudoloris* than Fahlbusch (1995) envisaged.

According to the stratigraphic ranges of the taxa in the cladogram, the *Vectipithex* clade separated from that comprising *Microchoerus*, *Necrolemur*, *N. filholi*, and '*N*'. *zuccolae* no later than the Early Eocene (Fig. 5). The implication is a phase of very rapid evolution within the subfamily in the first few million years of the Eocene comparable with the pattern seen in anaptomorphine omomyids in North America (Rose and Bown 1986), but of which little is still yet known. The most important synapomorphy of *Vectipithex* is loss of P2. The specialised anterior dentition developed on the resultant dental formula (see Occlusion section above; Thalmann 1994). Evolutionary trends in *Vectipithex* involved size increase; an elongation of the anterior dentition, with an increase in procumbency and a reduction in size of the P3 protocone; increase in the length-width proportions of the upper molars, reduction of the *Nannopithex* fold, and strengthening of the lingual cingulum; and transformation of the m1 paraconid from cuspate to crestiform.

## ACKNOWLEDGMENTS

We thank the following: J. and M. Smith, the National Trust, and English China Clays for access to sites; M. E. Collinson, A. P. Currant, A. C. and A. R. Milner, D. J. and A. Ward for help with field work; M. Godinot, D. E. Russell (MNHN), K. Heissig, G. R. Rössner (BSPG), E. Heizmann (SMNS), L. Loeffler (BU), H. Haubold, and G. Krumbiegel (GMH) for access to collections in their care; V. Fahlbusch, M. Godinot, and D. E. Russell for providing casts of important specimens; and A. Ball and L. Howard for SEM facility support.

## LITERATURE CITED

Bosma, A. A. 1974. Rodent biostratigraphy of the Eocene-Oligocene transitional strata of the Isle of Wight. Utrecht Micropalaeontological Bulletins 1:1–128.

Bremer, K. 1994. Branch support and tree stability. Cladistics 10: 295–304.

Brunet, M., J. L. Franzen, M. Godinot, J. J. Hooker, S. Legendre, N. Schmidt-Kittler, and M. Vianey-Liaud. 1987. European reference levels and correlation tables. Münchner Geowissenschaftliche Abhandlungen (A) 10:13–31.

Butler, P. M. 1973. Molar wear facets of early Tertiary North American primates; pp. 1–27 in M. R. Zingeser (ed.), Craniofacial Biology of Primates. Symposia of the Fourth International Congress of Primatology, Portland, Oregon, August 15–18, 1972, 3, S. Karger, Basel.

Chantre, E., and C. Gaillard. 1897. Sur la faune du gisement sidérolithique éocène de Lissieu (Rhône). Compte Rendu Hebdomadaire des Séances de l'Académie des Sciences, Paris 125:986–987.

Daley, B. 1999. Palaeogene sections in the Isle of Wight. A revision of their description and significance in the light of research undertaken over recent decades. Tertiary Research 19:1–69.

Edwards, N., and B. Daley. 1997. Stratigraphy of the Totland Bay Member (Headon Hill Formation, Late Eocene) at Hordle Cliff, Hampshire, southern England. Tertiary Research 18:35–50.

Fahlbusch, V. 1995. Ein neuer Primate (Mammalia, Omomyidae) aus dem marinen Ober-Eozän des inneralpinen Tertiärs von Oberaudorf nördlich Kufstein. Neues Jahrbuch für Geologie und Paläontologie Abhandlungen 198:15–26.

Filhol, H. 1873. Sur un nouveau genre de lémurien fossile, récemment découvert dans les gisements de phosphate de chaux du Quercy. Comptes Rendus Hebdomadaires des Séances de l'Académie des Sciences, Paris 77:1111–1112.

Gingerich, P. D. 1977. Dental variation in Early Eocene *Teilhardina belgica*, with notes on the anterior dentition of some early Tarsiiformes. Folia Primatologica 28:144–153.

Godinot, M., D. E. Russell, and P. Louis. 1992. Oldest known *Nannopithex* (Primates, Omomyiformes) from the Early Eocene of France. Folia Primatologica 58:32–40.

Gradstein, F.M., J.G. Ogg, and A.G. Smith, eds., 2004, A Geologic Time Scale 2004. Cambridge University Press, Cambridge, 589 pp.

Gregory, W. K. 1915. On the classification and phylogeny of the Lemuroidea. Bulletin of the Geological Society of America 26: 426–446.

Gunnell, G. F., and K. D. Rose. 2002. Tarsiiformes: evolutionary history and adaptation; pp. 45–82 in W. C. Hartwig (ed.), The primate fossil record. Cambridge University Press, Cambridge.

Heller, F. 1930. Die Säugetierfauna der mitteleozänen Braunkohle des Geiseltales bei Halle a.S. Jahrbuch des Halleschen Verbands für die Erforschung der Mitteldeutschen Bodenschätze und ihrer Verwertung (NF) 9:13–41.

Hooker, J. J. 1986. Mammals from the Bartonian (middle/late Eocene) of the Hampshire Basin, southern England. Bulletin of the British Museum (Natural History), Geology Series, 39:191–478.

Hooker, J. J. 1987. Mammalian faunal events in the English Hampshire Basin (late Eocene—early Oligocene) and their application to European biostratigraphy. Münchner Geowissenschaftliche Abhandlungen (A) 10:109–116.

Hooker, J. J. 1989. British mammals in the Tertiary period. Biological Journal of the Linnean Society 38:9–21.

Hooker, J. J. 1992. British mammalian paleocommunities across the Eocene-Oligocene transition and their environmental implications; pp. 494–515 in D. R. Prothero, and W. A. Berggren (eds), Eocene-Oligocene Climatic and Biotic Evolution. Princeton University Press, Princeton.

Hooker, J. J. 1996. Mammals from the Early (late Ypresian) to Middle (Lutetian) Eocene Bracklesham Group, southern England. Tertiary Research 16:141–174.

Hooker, J. J., M. E. Collinson, and N. P. Sille. 2004. Eocene-Oligocene mammalian faunal turnover in the Hampshire Basin, UK: calibration to the global time scale and the major cooling event. Journal of the Geological Society, London 161:1–12.

Hooker, J. J., E. Cook, and M. J. Benton. 2005. British Tertiary fossil mammal GCR sites; pp. 67–124 in M. J. Benton, E. Cook, and J. J. Hooker (eds), Mesozoic and Tertiary Fossil Mammals and Birds of Great Britain. Geological Conservation Review Series, No. 32, Joint Nature Conservation Committee, Peterborough.

Hooker, J. J., M. E. Collinson, P. F. Van Bergen, R. L. Singer, J. W. de Leeuw, and T. P. Jones. 1995. Reconstruction of land and freshwater palaeoenvironments near the Eocene-Oligocene boundary, southern England. Journal of the Geological Society, London 152: 449–468.

Köhler, M., and S. Moyà-Solà. 1999. A finding of Oligocene primates on the European continent. Proceedings of the National Academy of Sciences 96:14,664–14,667.

Lemoine, V. 1878. Communication sur les ossements fossiles des terrains tertiaires inférieures des environs de Reims faite à la Société d'Histoire Naturelle de Reims. Bulletin de la Société d'Histoire Naturelle de Reims 2:90–113.

Linnaeus, C. 1758. Systema naturae per regna tria naturae, secundum classes, ordines, genera, species, cum characteribus, differentiis, synonymis, locis. tenth edition, vol. 1. Laurentii Salvii, Stockholm, 824 pp.

Lydekker, R. 1887. Catalogue of the fossil Mammalia in the British Museum, (Natural History), part 5. British Museum (Natural History), London, 345 pp.

Matthews, S. C. 1973. Notes on open nomenclature and on synonymy lists. Palaeontology 16:713–719.

Ni, X.-J., Y.-Q. Wang, Y.-M. Hu, and C.-K. Li. 2004. A euprimate skull from the early Eocene of China. Nature 427:65–68.

Remy, J. A., J.-Y. Crochet, B. Sigé, J. Sudre, L. de Bonis, M. Vianey-Liaud, M. Godinot, J.-L. Hartenberger, B. Lange-Badré and B. Comte. 1987. Biochronologie des phosphorites du Quercy: mise au jour des listes fauniques et nouveaux gisements de mammifères fossiles. Münchner Geowissenschaftlicher Abhandlungen (A) 10: 169–188.

Richard, M. 1940. Nouveaux mammifères fossiles dans le Ludien supérieur de Pont d'Assou. Bulletin de la Société d'Histoire Naturelle de Toulouse 75:252–259.

Rose, K. D., and T. M. Bown, 1986. Gradual evolution and species discrimination in the fossil record. Contributions to Geology, University of Wyoming, Special Papers 3:119–130.

Rose, K. D., A. C. Walker, and L. L. Jacobs. 1981. Function of the mandibular tooth comb in living and extinct mammals. Nature 289: 583–585.

Schmidt, N. 1969. Eine alttertiäre Spaltenfüllungen von Ehrenstein westlich Ulm. Mitteilungen der Bayerischen Staatssammlung für Paläontologie und historische Geologie 9:201–208.

Schmidt-Kittler, N. 1971. Ein unteroligozäne Primatenfauna von Ehrenstein bei Ulm. Mitteilungen der Bayerischen Staatssammlung für Paläontologie und historische Geologie 11:171–204.

Schmidt-Kittler, N. 1977. Neue Primatenfunde aus unteroligozänen Karstspaltenfüllungen Süddeutschlands. Mitteilungen der Bayerischen Staatssammlung für Paläontologie und historische Geologie 17:177–195.

Simons, E. L. 1961. Notes on Eocene tarsioids and a revision of some Necrolemurinae. Bulletin of the British Museum (Natural History) 5:45–69, pls. 12–14.

Stehlin, H. G. 1916. Die Säugetiere des schweizerischen Eocaens. Critischer Catalog der materialien. *Caenopithecus—Necrolemur—Microchoerus—Nannopithex—Anchomomys—Periconodon—Amphichiromys—Heterochiromys*—Nachträge zu *Adapis*—Schlussbetrachtungen zu den Primaten. Abhandlungen Schweizerischen Paläontologischen Gesellschaft 41:1299–1552.

Swofford, D. L. 2000. PAUP*. Phylogenetic Analysis Using Parsimony (*and other methods). Version 4. Sinauer, Sunderland, Massachusetts.

Szalay, F. S., and E. Delson. 1979. Evolutionary History of the Primates. Academic Press, New York, 580 pp.
Teilhard de Chardin, P. 1927. Les mammifères de l'Eocène inférieur de la Belgique. Mémoires du Musée Royal d'Histoire Naturelle de Belgique 36:1–33.
Thalmann, U. 1994. Die Primaten aus dem eozänen Geiseltal bei Halle/Saale (Deutschland). Courier Forschungsinstitut Senckenberg 175: 1–161.
Trouessart, E. L. 1879. Catalogue des mammifères vivants et fossiles. Insectivores. Revue et Magasin de Zoologie Pure et Appliquée, Paris (3) 7:219–285.
Weigelt, J. 1933. Neue Primaten aus den mitteleozänen (oberlutetischen) Braunkohle des Geiseltals (geborgen 1932 in der Gruben Cecilie und Leonhardt). Nova Acta Leopoldina (NF) 1:97–156.
Wood, S. V. 1844. Record of the discovery of an alligator with several new mammalia in the freshwater strata at Hordwell. Annals and Magazine of Natural History (1) 14:349–351.
Wood, S. V. 1846. On the discovery of an alligator and of several new Mammalia in the Hordwell Cliff, with observations upon the geological phenomena of that locality. London Geological Journal 1: 1–7, pls 1–2.

Submitted August 15, 2007; accepted February 10, 2008.

APPENDIX 1. Description of numbered characters used in the character-taxon matrix.

All multistate characters are ordered since they are morphological transformation series. Outgroup states for *Teilhardina* are based almost entirely on *T. belgica*. The states of dental characters 2, 3, 4, and 5, however, are unknown for *T. belgica*. They are therefore established thus: character 2 by extrapolating from alveolar morphology of *T. belgica* (see Gingerich 1977); character 3 according to majority representation in the Microchoerinae; and characters 4 and 5 from *Teilhardina asiatica* (Ni et al. 2004). Included are relevant characters from Hooker (1986, 2007) and Thalmann (1994). Some characters from Thalmann (1994) are modified in light of intraspecific variation in *V. raabi*.

(1) i1 small, lower canine large (0); i1 large, lower canine small (1). N.B. The states of the two tooth types seem intimately linked, so they are treated as one character to avoid overweighting.
(2) Long axis of i1 at about 50 degrees to basal cheek tooth plane (=horizontal) (0); about 40 degrees or less (1). N.B. I1 angle probably follows that of i1 and is not treated as a separate character.
(3) I2 less than 1.4 times as long as wide (0); more than 1.4 times as long as wide (1).
(4) Upper canine more than half as wide as long (0); less than half as wide as long (1).
(5) Lower canine about 1.6 times as long as wide (0); approximately twice as long (1).
(6) P2 present (0); absent (1).
(7) P3 protocone position mesiolingual (0); nearly central lingually (1).
(8) P3 protocone more than half the height of the paracone (0); less than half (1).
(9) P3 protocone lobe 'waisted' (0); not 'waisted' (1).
(10) P3 with weak postparacrista (0); strong (1).
(11) P3 wider than long (0); approximately equidimensional (1); longer than wide (2).
(12) P3–4 without crest between paracone and protocone (0); with crest (1).
(13) P3–4 and more mesial upper teeth without mesiolingual crest (0); with crest (1).
(14) p1 present, squeezed buccally, p2 1-rooted, p3 2-rooted (0); p1-2 absent, p3 1-rooted (1).
(15) p3 nearly as large as p4 (0); smaller (1); very small (2) .
(16) p3 nearly as wide as long (0); c.1.5 times as long as wide (1).
(17) p4 with talonid long (0); short (1).
(18) p4 distal wall slopes occlusodistally, with small near vertical contact with m1 (0); is vertical, with more extensive sloping contact with m1 (1).
(19) p4 not inflated (0); inflated (1).
(20) p4 paraconid low (0); intermediate (1); high (2).
(21) p4 in lingual view symmetrical (0); obliquely canted mesially (1).
(22) p4 short and erect (0); long and procumbent (1).
(23) p4 metaconid present (0); absent (1).
(24) Molar crown height low (0); intermediate (1); high (2).
(25) Upper molar postprotocrista broken (0); scalloped (1); entire (2).
(26) Upper molar *Nannopithex* fold absent (0); present on M3 (1); present on M2–3 (2); present on M1-3 (3).
(27) Average upper molar length less than 63% width (0); 65-73% (1); 75–80% (2); more than 80% (3).
(28) M1–2 without lingual cingulum (0); with interrupted lingual cingulum (1); with complete lingual cingulum (2).
(29) M1–2 lingual profile tapering/rounded, postcingulum present (0); lingual profile tapering/rounded, with hypocone shelf (1); lingual profile tapering/rounded, with small hypocone only on M1 (2); lingual profile squared with distinct small hypocone on M1–2 (3); with hypocone as large as protocone on M1–2 (4).
(30) M1–2 with distinct postcingulum and metacingulum (0); fused to form distal cingulum (1).
(31) M1–2 postmetacrista long (0); short (1).
(32) M1–2 postmetacrista distobuccally orientated (0); nearly distally orientated (1).
(33) M2 tapering distally (0); not tapering distally (1).
(34) M3 crown and m3 talonid narrow (0); wide (1).
(35) m1–2 entoconid lower than hypoconid (0); as tall as hypoconid (1).
(36) m1 trigonid closed lingually (0); open (1).
(37) m1 paraconid lingual (0); median or more buccal (1).
(38) m1 paraconid cuspate (0); crestiform (1).
(39) m1 without mesial metaconid crest (0); with crest (1).
(40) m2–3 back of trigonid steep (0); vertical (1).
(41) m2–3 metaconid with smooth mesial face (0); with accessory cuspule in some individuals (1); consistently with accessory cuspule (2).
(42) m2–3 paraconid lingually situated (0); near median or more buccal (1).
(43) m2 paraconid strong (0); weak (1).
(44) m2 talonid approximately the same width as trigonid (0); wider (1).
(45) Basal plane of m3 trigonid and talonid aligned (0); angled up (1). N.B., This character is somewhat variable but is coded according to majority representation.
(46) m3 entoconid not salient lingually (0); salient lingually (1).
(47) m3 hypoconulid lobe narrow (0); wide (1).
(48) Enamel wrinkling absent (0); variable in presence and strength (1); consistent and strong (2).
(49) Anterior edge of ascending ramus steep (0); with shallow slope (1).

APPENDIX 2. Character-taxon matrix used in the phylogenetic analysis.

| | 0000000001 | 1111111112 | 2222222223 | 3333333334 | 444444444 |
|---|---|---|---|---|---|
| | 1234567890 | 1234567890 | 1234567890 | 1234567890 | 123456789 |
| *Teilhard.* | 0000000000 | 0000000000 | 0001100010 | 0000000000 | 000000000 |
| *Melan.* | ??????0100 | 0001200101 | 0000100000 | 10?0010001 | 10001000? |
| *Pseudol.* | 1000100100 | 1001110102 | 1101202030 | 0011111101 | 011010001 |
| *Paraloris* | ?????????? | ??????0000 | 0001?????? | ???0001001 | 011000001 |
| *N. zuccol.* | 1100000101 | 0101201112 | 1001131001 | 1111010001 | 21010111? |
| *N. filholi* | 10??000110 | 0111101102 | 1101131131 | 1111010010 | 211101110 |
| *Necrolem.* | 1000100110 | 1111001102 | 1101033041 | 1111000010 | 211101120 |
| *Microch.* | 1000000010 | 0111001102 | 1101033041 | 1111000010 | 211001120 |
| *N. humili.* | 11??0????? | ???1211112 | 1011?????? | ???1111001 | 010001010 |
| *V. raabi* | 1100010101 | 0001211112 | 1002131121 | 1111011001 | 210011010 |
| *V. quaylei* | 1?11011100 | 1001?11102 | 1101221121 | 10110????1 | 21101101? |
| *V. smith.* | 1111011100 | 2001211102 | 1101212221 | 1111011101 | 21101101? |
| *V. ulmens.* | ??????1100 | 200??????? | ???1212221 | 11?1011100 | ?110?101? |

**Abbreviations**: *humili.*, *humilidens*; *Melan.*, *Melaneremia*; *Microch.*, *Microchoerus*; *N.*, *Nannopithex*; *Necrolem.*, *Necrolemur*; *Pseudol.*, *Pseudoloris*; *smith.*, *smithorum*; *Teilhard.*, *Teilhardina*; *ulmens.*, *ulmensis*; *zuccol.*, *zuccolae*.